Journal of Advanced Research 37 (2022) 279–290

Contents lists available at ScienceDirect

Journal of Advanced Research

journal homepage: www.elsevier.com/locate/jare

Pegylation of phenothiazine – A synthetic route towards potent anticancer drugs

Sandu Cibotaru [a], Valentin Nastasa [b], Andreea-Isabela Sandu [a], Andra-Cristina Bostanaru [b], Mihai Mares [b], Luminita Marin [a,*]

[a] Petru Poni" Institute of Macromolecular Chemistry of Romanian Academy, Iasi, Romania
[b] Ion Ionescu de la Brad" University, Laboratory of Antimicrobial Chemotherapy, Iasi, Romania

HIGHLIGHTS

- Antitumor activity of two PEGylated phenotiazines was investigated
- The compounds showed cytotoxic activity against six tumor lines
- They inhibited the tumor growth in experimental mice
- The PEGylation improved the phenothiazine biocompatibility
- A synergistic effect of PEG and phenothiazine toward properties improvement was proved

GRAPHICAL ABSTRACT

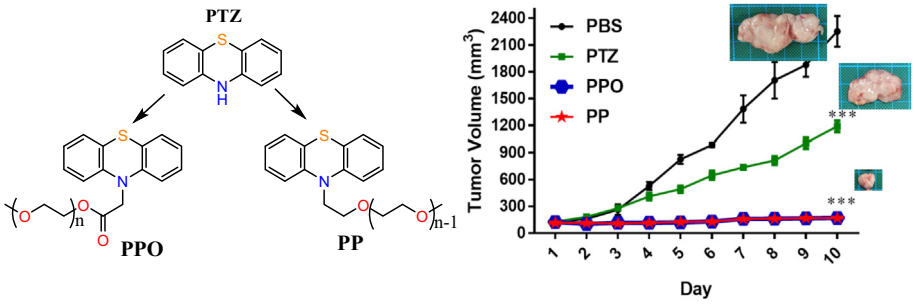

ARTICLE INFO

Article history:
Received 13 March 2021
Revised 1 July 2021
Accepted 6 July 2021
Available online 9 July 2021

Keywords:
Phenothiazine
Poly(ethylene glycol)
Tumour growth inhibition

ABSTRACT

Introduction: Cancer is a big challenge of the 21 century, whose defeat requires efficient antitumor drugs.
Objectives: The paper aims to investigate the synergistic effect of two structural building blocks, phenothiazine and poly(ethylene glycol), towards efficient antitumor drugs.
Methods: Two PEGylated phenothiazine derivatives were synthetized by attaching poly(ethylene glycol) of 550 Da to the nitrogen atom of phenothiazine by ether or ester linkage. Their antitumor activity has been investigated on five human tumour lines and a mouse tumor line as well, by determination of IC50. The *in vivo* toxicity was determined by measuring the LD50 in BALB/c mice by the sequential method and the *in vivo* antitumor potential was measured by the tumours growth test. The antitumor mechanism was investigated by complexation studies of zinc and magnesium ions characteristic to the farnesyltransferase enzyme, by studies of self-aggregation in the cells proximity and by investigation of the antitumor properties of the acid species resulted by enzymatic cleavage of the PEGylated derivatives.
Results: The two compounds showed antitumor activity, with IC50 against mouse colon carcinoma cell line comparable with that of the traditional antitumor drugs 5-Fluorouracil and doxorubicin. The phenothiazine PEGylation resulted in a significant toxicity diminishing, the LD50 in BALB/c mice increasing from 952.38 up to 1450 mg/kg, in phenothiazine equivalents. Both compounds inflicted a 92% inhibition

Peer review under responsibility of Cairo University.
* Corresponding author.
E-mail address: lmarin@icmpp.ro (L. Marin).

https://doi.org/10.1016/j.jare.2021.07.003

of the tumour growth for doses much smaller than LD50. The investigation of the possible tumour inhibition mechanism suggested the nanoaggregate formation and the cleavage of ester bonds as key factors for the inhibition of cancer cell proliferation and biocompatibility improvement.
Conclusion: Phenothiazine and PEG building blocks have a synergetic effect working for both tumour growth inhibition and biocompatibility improvement. All these findings recommend the PEGylated phenothiazine derivatives as a valuable workbench for a next generation of antitumor drugs.

Introduction

Cancer, an affliction known to humanity for thousands of years, became the second leading cause of death with a continuous growing of incidence and mortality rate, predicted to grow by as much 70% in the next 20 years [1]. Occurring in a high variety of different types, it has been recognized that its increasing incidence is close interconnected with the technological development, becoming thus the big challenge of the 21 century [2]. To defeat cancer, many possible therapies were considered, from traditional medicine [3] to DNA transfection [4]. Nevertheless, chemotherapy demonstrated the most efficient results, despite the high frequency and severity of adverse effects and low success rate caused by the reduced selectivity of the clinical chemodrugs. In this view, the discoveries of new more effective antitumor drugs with lessen side effects remained a desideratum of the contemporary society.

Looking to the chemical structure of the antitumor drugs, many moieties promoted antitumor activity. Among them, phenothiazine heterocycle is a building block with versatile biologic activity, which confirmed cytotoxicity against some cancer lines [5]. It was postulated that its cytotoxicity can be selectively improved by structural modifications, mainly *via* substitution at the nitrogen atom [6,7]. Considering the biologic versatility of phenothiazine (such as analgesic, antipsychotic, immunosuppressive, anti-inflammatory, bactericide, fungicide, antimalarial, antifilarial, trypanocidal, anticonvulsant), it can be envisaged that it may represents a valuable building block for the development of multifunctional anticancer drugs [8]. On the other hand, polyethylene glycol, a synthetic polymer approved by FDA for indwelling bioapplications, proved significant improvement of the pharmaceutical value of antitumor drugs [9]. This was possible due to its ability to enhance the retention time by protection against various degradation mechanisms which are active inside the tissues or cells. Besides, PEG has no interaction with the blood components, because very low plasma protein affinity [10].

Starting from these premises, our group designed PEGylated phenothiazine derivatives as new building blocks for anticancer drugs. PEG has been bonded to the phenothiazine heterocycle at the nitrogen atom and the cytotoxicity of the resulted compounds was investigated on normal cells and six tumour lines. It was demonstrated that the simple linking of PEG to phenothiazine lead to the enhancement of the cytotoxicity against the tumour cells compared to normal cells. Moreover, the *in vivo* investigation on experimental tumours in mice demonstrated that the studied PEGylated phenothiazines inhibited the tumour growth, promising to be a valuable workbench towards a new generation of more friendly multifunctional antitumor drugs.

Experimental

Materials

Phenothiazine 98%, ethyl bromoacetate 98%, sodium hydride 95%, methoxy poly(ethylene glycol) (550 Da, polymerization degree: 11–13), p-toluenesulfonyl chloride 98%, pyridine 99.8%, triethylamine (TEA) 99%, *N*-hydroxysuccinimide (NHS) 98%, *N*-(3-dimethylaminopropyl)-*N′*-ethylcarbodiimide hydrochloride (EDC. HCl) 98%, sodium hydroxide 97%, magnesium acetate tetrahydrate 99% and zinc acetate dehydrate 98% were purchased from Aldrich and 4-(dimethylamino)-pyridine 98% from Merck. All the reagents and solvents were used as received.

Materials for *in vitro* tests: normal human dermal fibroblasts (NHDF) cells were purchased from PromoCell (Heidelberg, Germany), MeWo, HOS, HeLa, MCF7 and HepG2 cells from CLS Cell Lines Service GmbH (Eppelheim, Germany), CT26 cells from Life Science Institute, National University of Singapore, Eagle's Minimal Essential Medium alpha (aMEM), Dulbecco's Modified Eagle Medium (DMEM) without phenol red and Penicillin–Streptomycin–Amphotericin B mixture (10 K/10 K/25 μg in 100 mL) from Lonza (Verviers, Begium), fetal bovine serum (non-USA origins) from Sigma Aldrich (Schnelldorf, Germany), TrypLE™ Express Enzyme and StemProAccutase from Gibco (Langley, Virginia, USA), LIVE/DEAD Viability/Cytotoxicity Kit and phosphate buffered saline (PBS) from Invitrogen (Eugene, Oregon, USA), CellTiter 96® Aqueous One Solution Cell Proliferation Assay (MTS) from Promega (Madison, Wisconsin, USA), CytoOne® 96-well plates from StarLab (Hamburg, Germany).

Synthesis

The compounds under study were synthesized using protocols from our previous study [11]. Briefly, the synthesis of 10-(methoxy poly(ethylene glycol))-10*H*-phenothiazine (**PP**) was realized by N-alkylation of phenothiazine with 2-methoxy poly (ethylene glycol) 4-methylbenzenesulfonate in DMF, using sodium hydride for phenothiazine deprotonation [11]. The product was purified by column chromatography (DCM:methanol 10:1, v/v), giving a deep red viscous liquid. **FT-IR** (KBr, cm^{-1}): 3060 (νCH aromatic), 2870 (νCH aliphatic), 1593, 1570 (νC = C), 1460 (δCH_2), 1292 (νC-N), 1110 (νC-O-C), 755 (δC-H); **^{1}H NMR** (400 MHz, DMSO d_6, ppm) δ = 7.22–7.13 (t,d, 4H, H1, H2, H8, H9), 7.06–7.04 (d, 2H, H4, H6), 6.97–6.93 (t, 2H, H3, H7), 4.07–4.04 (t, 2H, *H*11), 3.76–3.73 (t, 2H, H12), 3.50–3.42 (m, 48H, H13, H14), 3.24 (t, 3H, H15).

The synthesis of methoxy poly(ethylene glycol) 2-(10*H*-phenothiazin-10-yl) acetate (**PPO**) was realized by an esterification reaction of the 2-(10*H*-phenothiazin-10-yl) acetic acid with methoxy poly(ethylene glycol) in DCM, in the presence of DMAP and DCC [11]. The product was purified by column chromatography (DCM/methanol, 10/1, v/v), when an orange viscous liquid was obtained. **FT-IR** (KBr, cm-1): 3097–3063 (νCH aromatic), 2904 (νCH_3), 2875 (νCH_2), 1742 (νC = O), 1592–1560 (νC = Car), 1467 (δCH_2) 1193 (νC-O-C), 1109 (νC-O-C). **^{1}H NMR** (400 MHz, $CDCl_3$, ppm) δ = 7.10–7.07 (m, 4H, H1, H2, H8, H9), 6.92 – 6.89 (t, 2H, H3, H7), 6.62–6.60 (d, 2H, H4, H6), 4.55 (s, 2H, *H*11), 4.42–4.40 (t, 2H, H13), 3.74–3.71 (t, 2H, H14), 3.65–3.60 (m, 30H, H15, H16), 3.37 (s, 3H, H17);

Equipment and methods

NMR spectra were obtained on a Bruker Avance DRX 400 MHz spectrometer equipped with a 5 mm QNP direct detection probe and z-gradients, at room temperature, with an accumulation of 64 scans. The chemical shifts were reported as δ values (ppm) relative to the residual peak of the solvent.

Infrared spectra were recorded on a FTIR Bruker Vertex 70 Spectrometer, at room temperature, using KBr pellets.

The absorbance for CellTiter 96® Aqueous One Solution Cell Proliferation Assay (MTS) was measured using FLUOstar Omega Filter-based multi-mode microplate reader from BMG LABTECH (Offenburg, Germany).

Images for live/dead staining were acquired with a Leica DMI 3000B inverted microscope (Wetzlar, Germany). Live cells images, colored in green, were obtained using a GFP filter and dead cells images, coloured in red, using Texas Red (TX2) filter.

Cell culture: Cells were cultivated in complete MEM containing 1% Penicillin–Streptomycin–Amphotericin B mixture and 10% fetal bovine serum under 5% CO_2 humidified atmosphere at 37 °C. TrypLE™ Express Enzyme was used for passaging NHDF, HOS, HeLa, MCF7 and HepG2 cells. For passaging MeWo cells, StemProAccutase was used. Stock solutions for treatment were prepared with ultrapure water. Negative control cells were incubated only with complete cell culture medium.

*Preparation of the stock solutions for **in vitro** biologic testing:* The PEGylated compounds were dissolved in Ultra Pure Water (UPW) to obtain 5 mL solution of 100 mM. For this, 0.3655 g of PP, and 0.3955 g of PPO were weighed and then dissolved in UPW into a volumetric flask of 5 mL. The obtained solutions were subsequently divided into 20 vials (0.25 mL solution each) and lyophilized. The obtained solid probes were stored in the freezer at −15 °C to avoid eventually compound degradation. Before use, the compound from each vial was weighed again and the volume of the necessary UPW to obtain a 100 mM solution was recalculated for each vial.

In vitro *cytotoxicity assay*: The cytotoxicity was determined by MTS assay. The cells were seeded in 96-wells plates at densities of 10×10^3 cells/well for MeWo, HOS, HeLa and HepG2 cell line, 7×10^3 cells/well for MCF7 cell line and 5×10^3 cells/well for NHDF cell line in 100 μL aMEM medium/well and allowed to adhere for 24 h. After 24 h, the medium was replaced with the tested compounds solutions at various concentrations and the plates were incubated for another 48 h. Next, 20 μL MTS solution/well was added, 3 h prior to absorbance readings (λ = 490 nm) on a microplate reader. The relative cell viability is expressed as percentage of the viability of control (cells incubated only with cell culture medium) and the half maximal inhibitory concentration (IC_{50}) values were obtained from the analysis of absorbance data.

Data analysis was performed with GraphPad Prism software version 7.00 for Windows (GraphPad Software, San Diego, California). The obtained results represent the mean ± standard deviation (S.D.) of three different experiments. Statistical analysis was performed using multiple t tests (Holm-Sidak method). The difference was considered significant when $p < 0.05$.

A selectivity analysis was performed using the NHDF line as a control, to determine the cytotoxic selectivity of PP and PPO. The selectivity index was calculated with the following equation: SI = IC_{50} normal cell line / IC_{50} tumor cell line [12].

LIVE/DEAD Viability/Cytotoxicity. Qualitative cell viability assay was performed by using the LIVE/DEAD Viability/Cytotoxicity assay kit [13]. The cells were seeded in 96-well plates at densities of 10×10^3 cells/well for MeWo, HOS, HeLa and HepG2 cell line, 7×10^3 cells/well for MCF7 cell line and 5×10^3 cells/well for NHDF cell line in 100 μL a MEM medium/well and incubated for 24 h. Next, the medium was replaced with 100 μL of medium containing the tested compounds at a concentration equal with the IC50 value for each cell line. The cells were then incubated for 48 h, after which the medium was replaced with 100 μL LIVE/DEAD staining solution. The staining solution was obtained by combining 50 μL LIVE/DEAD 2X stock and 50 μL DMEM without phenol red. Images were acquired after 15 min of incubation at room temperature and processed with ImageJ Fiji distribution version 1.52a (National Institute of Health, USA) [14].

*Samples preparation for **in vivo** testing*: For the *in vivo* antitumor effect investigation, **PP** and **PPO** derivatives were dissolved in distilled water to obtain stock solutions of 20 mg/mL. For the calculation of the administration dose, the phenothiazine unit of the **PP** and **PPO** derivatives was considered the active substance. Pure phenothiazine, which was used as positive control, was dissolved in DMSO to obtain stock solution of 200 mg/mL. The doses for administrations were obtained by diluting the stock solutions in PBS to obtain 0.4 mL solution containing 2 mg active substance, meaning 100 mg active substance/kg bodyweight (Table 1). For LD50 testing, **PP** and **PPO** derivatives were solubilized in distilled water to obtain 100 mg/mL stock solutions.

Experimental design for the in vivo antitumor and toxicity testing: BALB/C mice were used to assess the antitumor effect and to determine median lethal dose LD50. The animals were purchased from the Cantacuzino Institute in Bucharest, 10-week-old nulliparous females, with an average weight of 20 ± 0.45 g. The acclimatization of the mice was done under identical conditions of temperature (22 ± 0.7 °C) and humidity (50 ± 10%), and the light/dark cycle provided was 12 h. Each experimental group was housed in autoclavable polycarbonate cages, 1500 cm^2, approximately 300 cm^2 /mouse. The animals had permanent access to water (ad libitum) (autoclavable bottles with drip system) and standardized food (provided by Cantacuzino Institute) with the following composition: 23% protein, 10% fat, 50% carbohydrates, 8% crude fiber and 9% vitamin-mineral premix, calcium carbonate and phosphate, amino acids. The animals were kept 7 days in the laboratory for accommodation and they were monitored daily to record any disease conditions and abnormal behaviour. Those that did not meet the required health criteria were removed from the experiment.

For the *determination of Lethal Dose 50 (LD50)* the sequential method has been used (UP and DOWN PROCEDURE-OECD 425). It was preferred because the number of animals is minimal and the estimated toxicity range is smaller. The method consists in the administration of a dose (d) to a single mouse. The dose was calculated in mg/kg and diluted in PBS to an intraperitoneal injection volume of 0.4 mL. If the mouse survived for 24–48 h (the monitoring interval was determined by the onset, duration and severity of toxic signs), another dose 1.3 times higher ($d \times 1.3$) was administrated to another mouse. If it also survived, it was continued with $d \times 1.3 \times 1.3 \ldots$, until the experimental animal died. If the first mouse dies, the test continued by decreasing the dose by 1.3 times (d/1.3), until reaching the dose at which the mouse lived. Testing stopped when 3 out of 5 mice survived consecutively at the upper limit. Any changes in behaviour and clinical manifestations were recorded. It was considered less likely to be an effect of treatment if: there was no obvious dose response, the measurement of the

Table 1
Protocol for administration of **PTZ**, **PP** and **PPO** compounds to BALB / C mice.

Group	Range of administration	No. of administrations	Dose: mg active substance i. e. PTZ /kg bodyweight
PBS	Once daily	10	–
PTZ			100 mg/kg; 2 mg/mouse
PP			100 mg/kg; 2 mg/mouse
PPO			100 mg/kg; 2 mg/mouse

endpoint being evaluated was inherently inaccurate, it was in a normal biological variation (e.g. within reference values), there was a lack of biological plausibility.

For *antitumor tests*, the animals were divided into 4 groups (5 mice/group), as follows: **Group PBS**: negative control group injected with phosphate buffer solution (PBS); **Group PTZ**: positive control group injected with phenothiazine (PTZ); **Group PP**: injected with **PP** derivative solution; **Group PPO**: injected with **PPO** derivative solution. All mice were acclimatized at least one week before the start of the experiment. CT26 colorectal cancer cells were transplanted on a growth medium [i.e., Dulbecco's Modified Eagle's Medium (DMEM) containing 10% Fetal Bovine Serum (FBS), 1 mM sodium pyruvate, 1% glutamine, and 1% streptomycin] for multiplication. Tumour cells were cultured at 37 °C and 5% CO_2. The inoculum was administered subcutaneously in the thoracic-dorsal (intrascapular) region of the mice anesthetized with 3% isoflurane, in a volume of 0.25 mL containing a number of 500 000 tumour cells. Prior to inoculation, the administration site was shaved and disinfected with povidone iodine. Then, the mice were monitored daily, to assess the degree of tumour development, their general condition, behaviour, respiration, recording the clinical score [15,16], the toxic effects of long-term administrations such as cyanosis, anorexia, and jaundice or any other sign of pain. All mice developed subcutaneous tumours. The tumour became palpable on day 5 after injection of CT26 cells. The *in vivo* antitumor test started in the day 7 after inoculation, when the tumour volume was around 120 mm^3.

The administration protocol was given in Table 1. All mice were injected intraperitoneally (IP) using a 27G insulin syringe, one administration daily, for 10 days. The dose was calculated considering the phenothiazine unit as active substance, 100 mg/kg bodyweight, meaning approximately 2 mg /mouse, respectively, e.g. 2 mg PTZ/mouse; 7.33 mg PP/mouse; 7.83 mg PPO/mouse. The compounds were diluted in PBS so that the final volume of the solution injected intraperitoneally was 0.4 mL/mouse [17,18]. Tumour measurements were performed daily before administration to establish a basis for comparison. The tumour volume was determined by measuring 3 diameters and subsequently calculated using the formula for a hemielipsoid: Volume = 0, 52 × L (length of the longest diameter) × W (width-diameter perpendicular to length) × H (height) [19].

In order to appreciate the efficiency of studied compounds compared to other findings reported in literature, *the percent of tumour growth inhibition* (Ti%) was calculated with the equation: $T_i\% = (1-\frac{D(d)}{D(c)})x100$, where D(d) – tumour dimension developed in the treated mice and D(c) - tumour dimension developed in the control mice.

Statistical analyses were performed using GraphPad Prism software version 7.00 for Windows (GraphPad Software, San Diego, California). The obtained results represent the mean ± standard deviation (S.D.) of three different experiments, and the differences between groups were done with 2 way ANOVA Tabular results and multiple comparisons. P-values < 0.05 were considered as significant (*p < 0.05, **p < 0.001,

***p < 0.0001), p > 0.05 the differences between data are not significant.

Ethical implications

The study was conducted in accordance with national and international regulations on animal welfare, identification, control and elimination of factors causing physiological and behavioural disorders: Directive EC86 / 609 EU; Government Ordinance no. 37/2002, approved by Law no. 471/2002; Law 205/2004 on animal protection, amended and supplemented by Law no. 9/2008; Joint Order of ANSVSA and of the Ministry of Interior and Administrative Reform no. 523/2008 for the approval of the Methodological Norms for the application of Law 205/2004 on animal protection.

Results and discussions

The paper focuses on the investigation of the antitumor activity of two PEGylated phenothiazine derivatives, for which PEG has been bonded to the phenothiazine by ether or ester unit (Scheme 1). It should be stressed that, following well established synthetic protocols, the compounds were obtained with high purity (higher than 99%). They presented excellent solubility in water and common organic solvents (Figure S1), and were hydrolytic stable on an investigation period of 7 days. However, a deeper investigation of their water solutions by DLS and UV–vis showed that they self-assembled into nanoaggregates, at the critical aggregation concentration of $8.7x10^{-4}$ and $9.23x10^{-4}$ mM for **PP** and **PPO** respectively (Figure S2, Figure S3) [11]. The hydrodynamic diameter of the nanoaggregates was dependent on the solution concentration, decreasing from 289 to 106 nm for **PP**, and from 322 to 63 nm for **PPO** when the concentration decreased from 10 to 0.1 mM, rationally explained by the variation of the molecules density which influenced the aggregate size, i.e. a higher molecules density favoured a higher aggregate size (Figure S2) [20].

In vitro investigation of the antitumor activity

The investigation of the antitumor activity of the **PP** and **PPO** derivatives was performed by determining the cytotoxicity on five human cancer cell lines: cervical carcinoma (HeLa); malignant melanoma (MeWo); osteosarcoma (HOS), breast cancer (MCF7) and liver cancer (HepG2) *versus* a normal cell line (NHDF). Having in mind the *in vivo* investigation of the antitumor activity on mice, mouse colon carcinoma cell line (CT26) was also included in the study. The cytotoxicity tests were done for solutions with concentration from 1 μM up to 1 mM, and the IC_{50} was determined for each cell line. The dose-responsive curves were represented in Fig. 1a-l, as graphs of the relative cell viability against the concentration of **PP** and **PPO**.

At first glance, it can be observed that among the human tumor cell lines, for the concentration of 64 μM at which the NHDF viability was around 80%, the **PP** showed the higher cytotoxic effect against MeWo (cell viability 47%), and the **PPO** against HeLa (cell viability 40%). Compared to the human cell lines, the viability of CT29 tumor cells decreased to<40% for a similar concentration of both **PP** and **PPO** compounds.

These observations were reflected in a more accurate way in the values of IC_{50} parameter, calculated for both compounds on every cell line (Fig. 1m, Table S1). It can be seen that **PP** and **PPO** exhibited high cytotoxic activity against CT26 cells, and IC_{50} values were 6 and 12 fold lower compared to that against NHDF cells indicating good selectivity. Even thought that CT26 cells are specific for mice

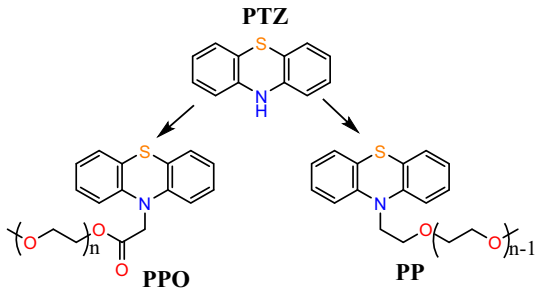

Scheme 1. Structure of the studied compounds and phenothiazine precursor.

tumours and not human ones, by comparing the results with other data reported for therapeutic antitumor drugs or other compounds investigated as potential anticancer drugs, the antitumor potency of **PP** and **PPO** compounds appears remarkable (Table 2). As an example, it can be seen that IC50 of **PP** and **PPO** is comparable with that of traditional antitumor drugs 5-Fluorouracil and doxorubicin, therefore encouraging further *in vivo* tests. Moreover, it should be remarked that even though some papers reported significant higher IC_{50} values, they did not report IC_{50} for normal cells, making difficult to appreciate their selectivity.

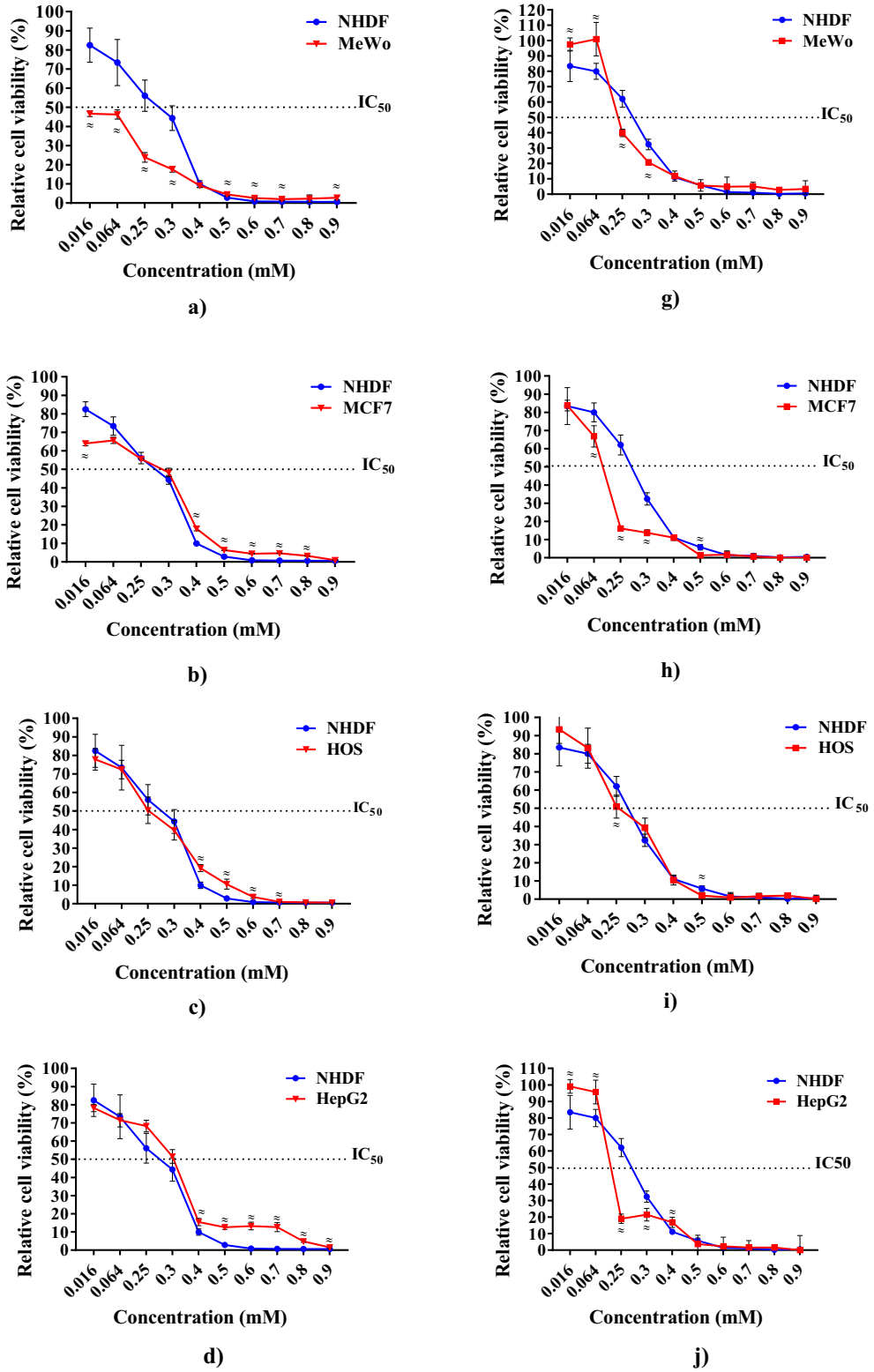

Fig. 1. Graphical representation of the relative cell viability of different human tumour lines and CT26 mouse tumour line when in contact with different concentrations of **PP** (a-f) and **PPO** (g-l) and graphical representation of the IC50 parameter (m) ≈: $p < 0.05$ for NHDF vs. tumour cell lines by multiple t tests, using the Holm-Sidak method.

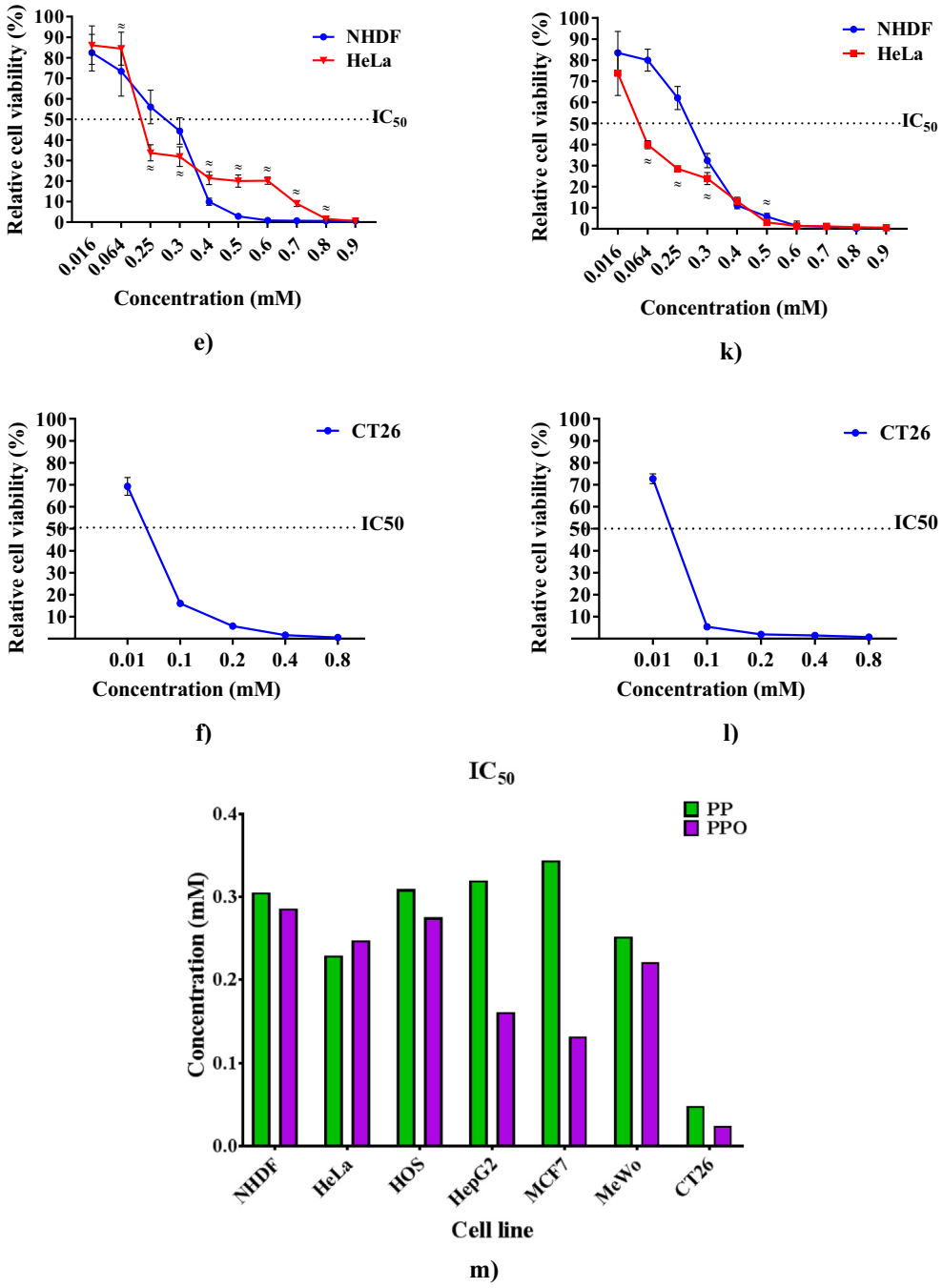

Fig. 1 (*continued*)

Regarding the IC_{50} values obtained on the human cell lines, **PP** have increased cytotoxic effect against two tumour lines, HeLa (cervical cancer) and MeWo (skin cancer), for which the IC_{50} gave values of 229.1 μM and 251.9 μM, respectively, compared to the 305.8 μM value obtained for the normal cell line. By comparison, **PPO** showed higher cytotoxic effect against all the investigated tumour cell lines compared to the normal cells, but significant lower IC50 values were recorded for HepG2 (human liver cancer) and MCF7 (breast cancer): 161.3 μM and 131.7 μM, respectively. These values were one third lower and one-half lower, respectively, compared to that for normal cells (286.2 μM). However, the selectivity index SI(IC50) calculated using NHDF as control showed low values indicating low selectivity (Table S2) [34,35]. Compared to traditional therapeutic drugs, IC50 values of **PP** and **PPO** were mostly higher and sometimes lower, encouraging further investigations (Table S3).

Fluorescent imaging confirmed the MTS assay results, as can be seen in Fig. 2, where live cells were stained an intense, uniform green, while dead cells had a predominantly nuclear red fluorescence [36]. Characteristics of apoptotic cells like cell shrinkage, rounding, partial detachment and lobulated appearance can be easily observed for HeLa, MCF7 and HepG2 cells treated with **PP**, and NHDF, MCF7 and HepG2 cells treated with **PPO** [37].

In vivo toxicity

In order to establish the doses for safe *in vivo* use of the **PP** and **PPO**, the *in vivo* toxicity of the compounds was investigated. Usu-

Table 2
Half maximal inhibition concentration (IC50) of some therapeutic antitumor drugs and other compounds determined on **CT26** tumour line.

Name	IC50 (μM)	Reference
PP	47.89	Present study
PPO	24.19	Present study
5-Fluorouracil	39.81	[21]
Doxorubicin	35	[22]
DOX-TOS-TPGS Vitamin E-based micelles loaded with doxorubicin	22.8	[22]
Simvastatin ([(1S,3R,7S,8S,8aR)-8-[2-[(2R,4R)-4-hydroxy-6-oxooxan-2-yl]ethyl]-3,7-dimethyl-1,2,3,7,8, 8a-hexahydronaphthalen-1-yl] 2,2-dimethylbutanoate)	5	[23]
Triamterene (6-phenylpteridine-2,4,7-triamine)	24.45	[24]
Napabucasin derivatives 2-acetylnaphtho[2,3-b]furan-4,9-dione derivatives	1–2	[25]
SORt f 4-{4-[({[4-chloro3-(trifluoromethyl-phenyl]amino}carbonyl)amino] phenoxy}-N-methylpyridine- 2-carboxamide tosylate	8.12	[26]
Tetrandrine 9,20,21,25-tetramethoxy-15,30-dimethyl-7,23-dioxa-15,30-diazaheptacyclo[22.6.2.2^{3,6}.1^{8,12}.1^{14,18}. 0^{27,31}.0^{22,33}]hexatriaconta-3,5,8(34),9,11,18,20,22(33),24(32),25,27(31),35-dodecaene	10	[27]
PTX-LMB loaded PLGA NPs Phenothiazine based compound	0.447	[28]
Pc9-T1107 sulfur-linked 2,9(10),16(17),23(24) tetrakis[(2-dimethylamino)ethylsulfanyl]phthalocyaninatozinc(II) + Poloxamine Tetronic 1107	0.370	[29]
1,3,4-oxadiazole derivatives 5-(bromomethyl)-3-phenyl-1,2,4-oxadiazole derivatives	3.6	[30]
CPP-modified gelonin cG-L: gelonin-LMWP chemical conjugate	2–0.005	[31]
5-Fluorouracil loaded liposomes	12.02	[32]
gold(I) complexes with 5-phenyl-1,3,4-oxadiazole-2-thione and phosphine	100–0,1	[33]

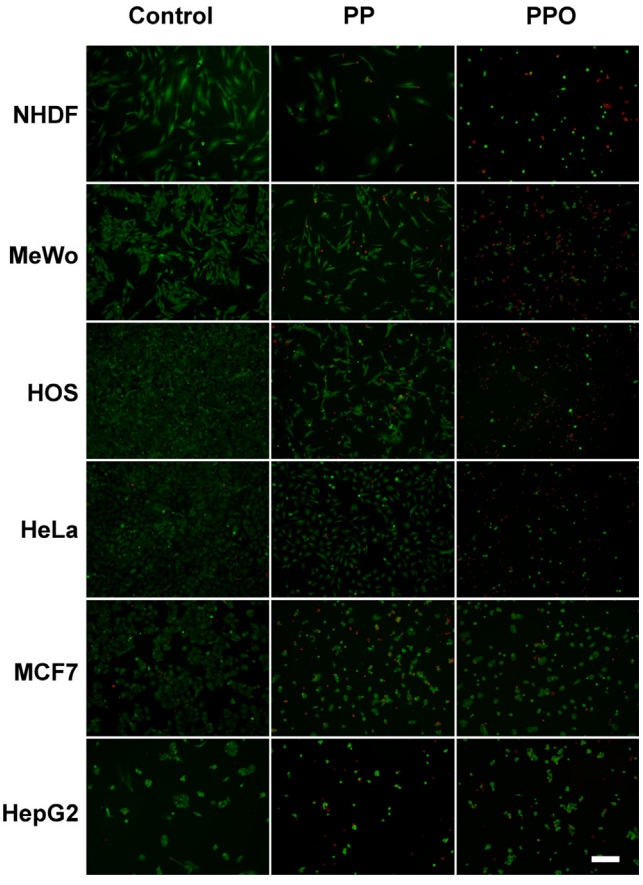

Fig. 2. Live/dead staining. Cells were treated for 48 h with concentrations equivalent with IC50 for each cell line and compound. Living cells were stained in green while dead cells, in red. The scale represents 200 μm.

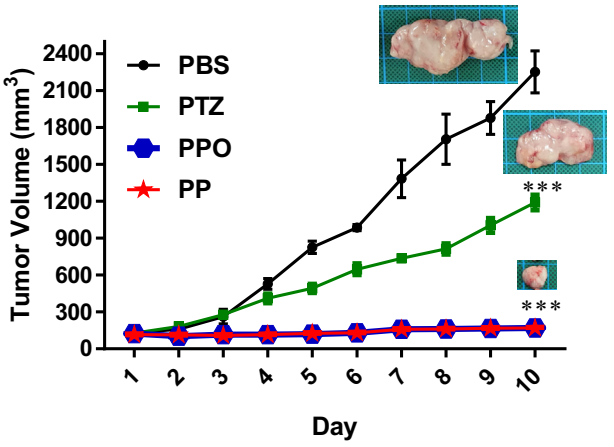

Fig. 3. Graphical representation of the tumour volume (mm^3) during the treatment and representative images of tumours after 10 days of treatment (***p < 0.0001).

ally, the estimation of the *in vivo* toxicity of a new substance is preliminary done by determining the acute toxicity - LD50, a dose that causes death in 50% of the studied experimental animals. After testing several dose levels for each compound, as single intraperitoneal administration, according to the protocol described in the Experimental part, it was concluded that the LD50 in BALB/c mice was 952.38 mg/kg for phenothiazine (**PTZ**) and increased to 1450 mg/kg for **PP** and 1300 mg/kg for **PPO** (Table S4). It should be highlighted that LD50 for **PP** and **PPO** was expressed as equivalent in phenothiazine (see Experimental part). It was obvious that PEGylation reduced the toxicity of the phenothiazine with>50%. Contrary to the *in vitro* findings, the *in vivo* toxicity of **PPO** was slightly higher compared to that of **PP**.

The mice in both **PP** and **PPO** groups exhibited serious adverse reactions, CNS depression, generalized muscle contractions with

Table 3
The inhibition of tumour growth in CT26 tumour-bearing mice.

Compound name	Structure	Ti (%)*	Reference
PTZ	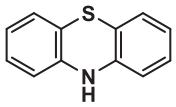	47	This study
PPO	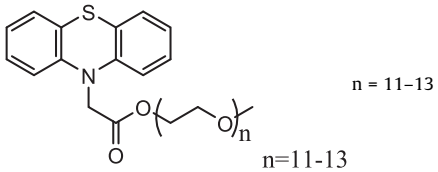 n = 11–13 n=11-13	92	This study
PP	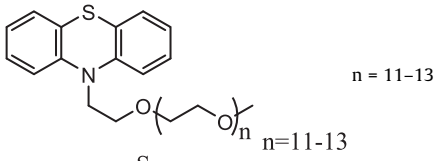 n = 11–13 n=11-13	92	This study
Thioridazine	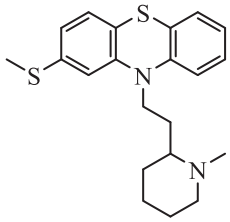	51	[42]
PTX-MB@PLGA	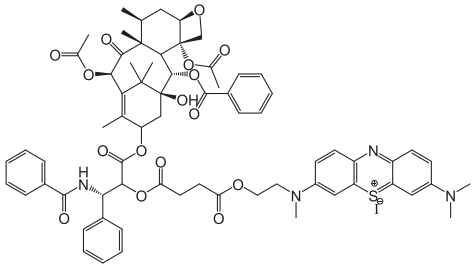	60	[28]
Doxorubicine	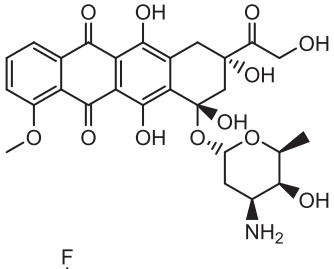	27.27	[43]
5-Florouracil	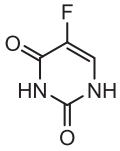	75, 82.85, 85.71	[44]

*T_i = percent of tumor inhibition during 10 days of treatment calculated with the eq. $T_i\% = (1-\frac{D(d)}{D(c)})x100$, where D(d) – tumour volume developed in the treated mice and D(c) - tumour volume developed in the control mice

body torsion, and reduced cardiac, respiratory, and central activity, immediately after administration (1–2 min) at all tested levels. These reactions last for 10 min, and then the mice recovered and adopted a normal behaviour. About 20–30 min after this return, a state of suffering occurred especially in the **PPO** group that leads to the partial immobilization of the animal. To a lesser extent, the phenomena were also observed in animals from the **PP** group, but they were of lower intensity. In the case of the phenothiazine group, a state of suffering accompanied by depression was recorded only at the highest dosage levels. The adverse effects described above are characteristic to the phenothiazine derivatives used as neuroleptic drugs or investigated as anticancer drugs [7,38], and were ascribed to the ability of the positively charged nitrogen to induce a higher permeability of the blood–brain-barrier (BBB) [39]. On the other hand, the amphiphilic character of the PEGylated phenothiazine derivatives allows the diffusion into the endothelial cells and from there to the brain [40]. This can be the indicative of a better absorption of the PEGylated derivatives, especially of the **PPO** in which the PEG chain has been bonded to the phenothiazine core by an ester linking group.

In vivo investigation of the antitumor activity

The next step in the investigation of the antitumor activity was to monitor the inhibitory effect of the phenothiazine derivatives on the tumour growth rate in mice as animal models. Starting from the idea

that systemic cytotoxic chemotherapy is still the therapeutic basis for many types of cancer, the compounds solutions were intraperitoneal administered one dose per day during 10 days, at doses much lower that LD50 [34,41]. The evolution of the tumour growth in model animals treated with phenothiazine was considered as a positive control and those treated with PBS as negative control. The obtained data are presented in Fig. 3 and Table S5.

In the first day of administration, the average volume of the subcutaneous tumours was around 120 mm^3 in all experimental groups. At the end of experiment, the tumour volume recorded in the negative reference (PBS group) increased about 17 times to 2253.72 mm^3. In the group treated with phenothiazine (PTZ group) as positive reference, the tumour increased about 9 fold higher (1190.12 mm^3) while in the groups treated with **PP** and **PPO** respectively, the tumour increased<1.5 times (173.49 mm^3 in the **PP** group and 170.58 mm^3 in the **PPO** group). This means that the tumour inhibitory (Ti) effect of the **PTZ** compared to the negative control PBS of 47%, drastically increased to 92% by PEGylation in the case of the mice treated with **PP** and **PPO**. Interesting, even if the *in vitro* tests indicated **PPO** as more effective than **PP** in killing the CT26 cells, the *in vivo* tests showed statistical insignificant differences between them ($p > 0.05$), possible due to different concentration of the compounds used for measurements.

To estimate the efficiency of the phenothizine PEGylation on the tumour growth inhibition, the percent of tumour inhibition (Ti) was compared with those of the other phenothiazine derivatives reported for CT26 cell line (Table 3), or other tumour lines (Table S6) for a similar treatment period. For comparison reasons, the results reported for some therapeutic anticancer drugs were included in Table 3 too. It can be seen that the tumour inhibition of 92% recorded for the studied PEGylated phenothiazines is significant higher compared to other Ti values, a maximum of almost 60% being reported for quite complicated phenothiazine structures [28]. Moreover, the CT26 tumour inhibition growth was significantly higher compared to 5-fluorouracyl and doxorubicine drugs. Considering the simple structure of the studied PEGylated phenothiazines, the lack of toxicity of the PEG building block, and the possibilities to further functionalize the phenothiazine core with potent anticancer units, we can consider that phenothiazine PEGylation is a valuable pathway for designing anticancer drugs.

Cumulating the data of the *in vivo* tests, it can be concluded that the PEGylated phenothiazine derivatives, especially **PP** one, have potential of anticancer drugs, and their design can serve as a work bench for further chemical engineering in order to improve the antitumor activity and to minimize the side effects, towards a new class of anticancer drugs.

Antitumor mechanism

To further develop the design of the PEGylated phenothiazines, it is important to understand the structure particularities triggering the improvement of antitumor activity and on the other hand those promoting toxicity. As the principal building blocks of the studied compounds are the phenothiazine and PEG, their influence was considered. Moreover, the presence of the ester bond in **PPO**, which can be easily hydrolysed under the influence of esterases to give the acid precursor (Scheme 2) was examined as well [45,46]. It should be mentioned that the esterases are overexpressed in the tumour cells increasing the probability of ester bond cleavage in their proximity [47].

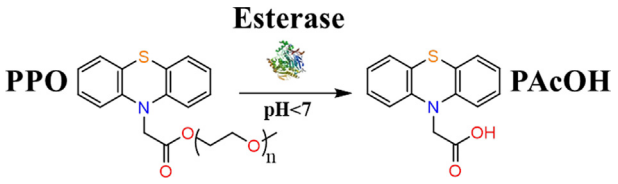

Scheme 2. Schematic representation of the possible enzymatic degradation of **PPO.**

Investigation of farnesyltransferase inhibition. The investigation of the antitumor activity of various phenothiazine based derivatives demonstrated that the mechanism of their tumour growth inhibition involves the inhibition of farnesyltransferase (FT) enzyme, which plays a key role in the tumour cell proliferation [48,49]. More precisely, the inhibition mechanism consists in the binding of thiol units or coordination of Zn^{2+} or Mg^{2+} sites of FT [50,51]. As no specific sites for binding thiol units were present in the structure of the studied PEGylated phenothiazines, their ability to inhibit FT was verified by experiments of complexation with Zn^{2+} or Mg^{2+} metals (see Supporting Information Figures S5-S11 and explanations therein). The phenothiazine product (PAcOH) which can result by enzymatic degradation of **PPO** (Scheme 2) was investigated too. Neither **PP** nor **PPO** were able to bind Zn^{2+} or Mg^{2+} ions, indicating their inability to inhibit FT. Nevertheless, **PAcOH** was able to bind both ions. In the case of magnesium, the bonding consisted in the formation of an ionic compound, were Mg^{2+} coordinated water molecules and the electron-donating phenothiazine played the role of counter ion neutralizing the magnesium charge (Fig. 4) [52]. In the case of zinc, it appeared that Zn^{2+} ions were coordinated by the acid groups of the **PAcOH**. This suggests that in biologic fluids which favour the **PPO** hydrolysis, the resulted **PAcOH** can inhibit the farnesyltransferase by bonding the magnesium and/or zinc sites. This hypothesis is in agreement with the higher *in vitro* antitumor activity of the **PPO** compared to **PP**.

Investigation of the PEGylation effect. Recent advances in the tumour therapy demonstrated that PEG is a great building block for enhancing the drugs efficiency by protecting them against var-

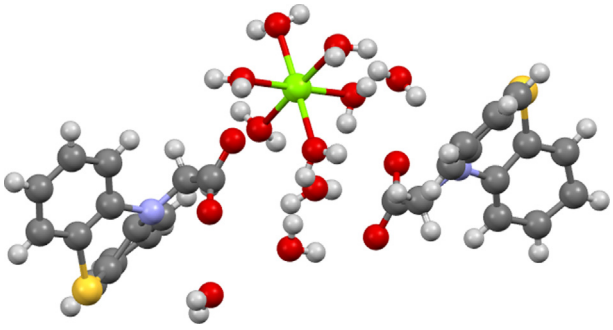

Fig. 4. Single crystal X-ray structure of the product obtained by mixing **PAcOH** with $Mg(Ac)_2$.

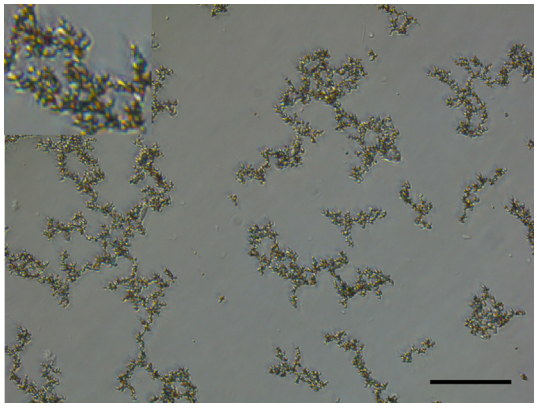

Fig. 5. Brightfield microscopy images of **PPO** in the blank medium (in the inset it was displayed a magnified region of the picture). The scale represents 100 μm.

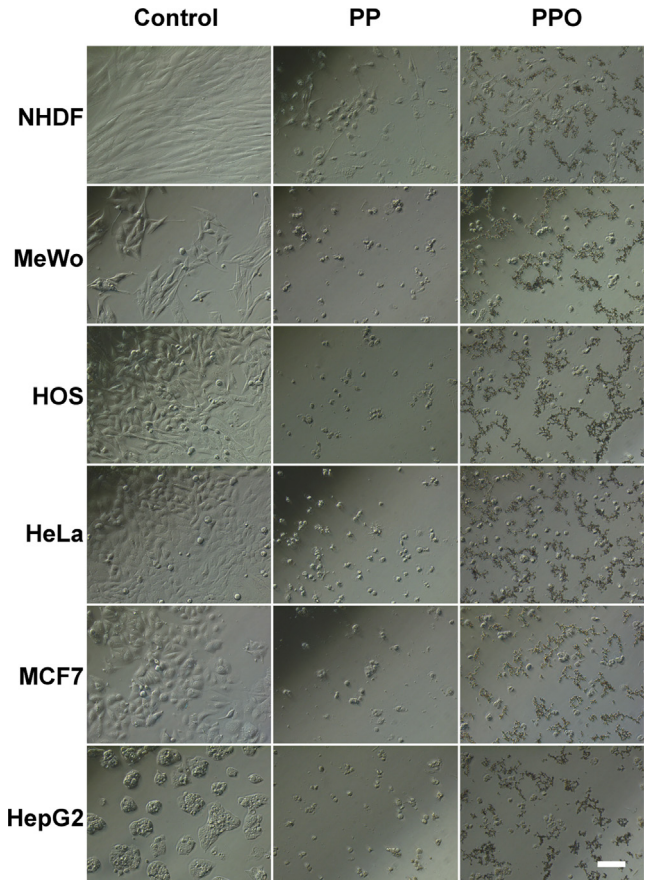

Fig. 6. **PP** and **PPO** behaviour in cell culture. The scale represents 100 μm.

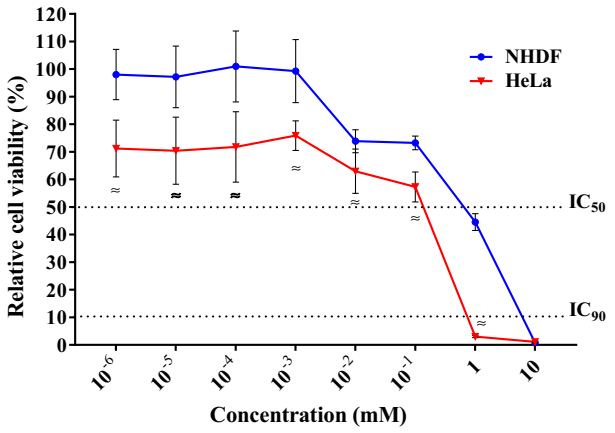

Fig. 7. Graphical representation of the relative cell viability of NHDF and HeLa cells when in contact with different concentrations of **PAcOH** (≈: $p < 0.05$ for NHDF vs. tumour cell lines by multiple t tests, using the Holm-Sidak method).

ious degradation mechanisms that are active inside the tissues or cells [53]. The investigation of studied PEGylated phenothiazines showed that PEG chains prompted the formation of nanoaggregates with a phenothiazine core protected by a PEG shell [11,54,55]. In this view, the **PPO** and **PP** in blank medium and in contact with various cells were analysed by brightfield microscopy. It was seen that **PPO** displayed clear birefringent nanoaggregates with tendency to agglomerate in the blank medium (Fig. 5, Figure S4).

Photos acquired during the *in vitro* testing indicated that **PPO** nanoaggregates had the tendency to accumulate in the proximity of the cells (Fig. 6). These results suggest that the antitumor effect of **PPO** is the result of a synergistic effect of the PEG and ester units. On a hand, the presence of PEG assures the phenothiazine protection inside the nanoaggregates improving its biocompatibility and on the other hand the ester units permit the enzymatic cleavage of the phenothiazine acid precursor which can inhibit the FT enzyme of the tumour cells [47]. This hypothesis is supported by the literature data which indicate that the cellular uptake of PEGylated derivatives follows a different mechanism compared to small molecule drugs. Thus, while the small drug molecules penetrate inside the cell by diffusion, the PEGylated compounds penetrate the cell membrane by endocytosis. In this process a vacuole is formed and the polymeric compound is degraded, in the case of **PPO** probably by the cleavage of the ester function. As a result, the **PAcOH** acid is formed and interacts with FT [56,57].

To further investigate the feasibility of this hypothesis, the antitumor activity of the **PAcOH** phenothiazine precursor was investigated on HeLa cells, for which **PPO** showed the best results. It was found that for a wide concentration range, from 10^{-6} to 10^{-3} mM, the viability of the normal cells was not affected while that of the tumour cells was around 70% (Fig. 7). This means that in the scenario of a slow release of the **PAcOH** by enzymatic degradation, the tumour cell killing occurs even for very low **PAcOH** concentrations. Moreover, the IC50 on HeLa cells was 13.2 μM while for NHDF cells was 498.5 μM, giving a high selectivity index of 37, indicating a high selectivity towards tumour cells.

Conclusions

The investigation of *in vitro* and *in vivo* antitumor activity of two PEGylated phenothiazine derivatives revealed a synergism of the phenothiazine and PEG building blocks towards an improved tumour inhibition. Thus, the two compounds showed half maximal inhibitory concentration against mouse colon carcinoma cell line (CT26) comparable with that of the traditional antitumor drugs 5-Fluorouracil and doxorubicin. The median lethal dose in BALB/c mice significantly increased from 952.38 mg/kg for phenothiazine to 1450 mg/kg and 1300 mg/kg (in phenothiazine equivalents) for PEGylated derivatives, highlighting the role of PEG in the biocompatibility improvement. Both compounds inflicted a 92% inhibition of the tumour growth compared with a maximum of 60% reported for other phenothiazine compounds with quite complicated chemical structures. Furthermore, the investigation of possible tumour inhibition mechanisms suggested that the binding of PEG to the phenothiazine *via* an ester linkage was favourable for (i) the nanoaggregate formation with protective role for phenothiazine units and (ii) enzymatic cleavage releasing the acid phenothiazine species, which inhibit farnesyltransferase, leading to the inhibition of the cancer cell proliferation. All these findings recommend the PEGylated phenothiazine derivatives as a valuable workbench for a next generation of antitumor drugs.

Compliance with ethics requirements

The study was conducted in accordance with national and international regulations on animal welfare, identification, control and elimination of factors causing physiological and behavioral disorders: Directive EC86 / 609 EU; Government Ordinance no. 37/2002, approved by Law no. 471/2002; Law 205/2004 on animal protection, amended and supplemented by Law no. 9/2008; Joint Order of ANSVSA and of the Ministry of Interior and Administrative Reform no. 523/2008 for the approval of the Methodological Norms for the application of Law 205/2004 on animal protection.

Credit author statement

L. Marin, M. Mares and S. Cibotaru contributed to the conception, design, analysis, interpretation, writing and critical revision of the manuscript. S. Cibotaru performed the synthesis of the compounds, their structural characterization, and investigation of the antitumor mechanism and drafting of the manuscript. V. Nastasa and A.C. Bostanaru performed the *in vivo* tests on BALB/c mice and drafted the manuscript. I.A. Sandu performed the *in vitro* tests of antitumor activity and drafted the manuscript. All authors gave final approval and agreed to be accountable for all aspects of the work.

Declaration of Competing Interest

The authors declare that they have no known competing financial interests or personal relationships that could have appeared to influence the work reported in this paper.

Acknowledgements

The paper was supported by a project financed through a Romanian National Authority for Scientific Research MEN – UEFISCDI, grant project PN-III-P4-ID-PCCF-2016-0050.

Appendix A. Supplementary data

Supplementary data to this article can be found online at https://doi.org/10.1016/j.jare.2021.07.003.

References

[1] Alexandrov LB, Kim J, Haradhvala NJ, Huang MN, Ng AWT, Wu Y, et al. The repertoire of mutational signatures in human cancer. Nature 2020;578:94–101.
[2] Tiwari AK, Roy HK. Progress against cancer (1971–2011): how far have we come? J Intern Med. 2012;271:392–9. doi: https://doi.org/10.1111/j.1365-2796.2011.02462.x.
[3] Xiang Y, Guo Z, Zhu P, Chen J, Huang Y. Traditional Chinese medicine as a cancer treatment: Modern perspectives of ancient but advanced science. Cancer Med. 2019;8:1958–75. doi: https://doi.org/10.1002/cam4.2108.
[4] Marin L, Ailincai D, Cahn M, Stan D, Constantinescu CA, Ursu L, et al. Dynameric Frameworks for DNA Transfection. ACS Biomater. Sci. Eng. 2016;2:104–11. doi: https://doi.org/10.1021/acsbiomaterials.5b00423.
[5] Varga B, Csonka Á, Csonka A, Molnár J, Amaral L, Spengler G. Possible biological and clinical applications of phenothiazines. Anticancer Res. 2017;37:5983–93. doi: https://doi.org/10.21873/anticanres.12045.
[6] I.M. Moisea, E. Bîcu, A. Farce. J. Dubois. A. Ghinet, Indolizine-phenothiazine hybrids as the first dual inhibitors of tubulin polymerization and farnesyltransferase with synergistic antitumor activity, Bioorg. Chem., 103 (2020) 104184. doi: 10.1016/j.bioorg.2020.104184.
[7] M. Otręba, L. Kośmider, In vitro anticancer activity of fluphenazine, perphenazine and prochlorperazine. A review, J. Appl. Toxicol. 41(2021) 82–94. doi: 10.1002/jat.4046.
[8] Morak-Mlodawska KP, Jeleń M. Recent progress in biological activities of synthesized phenothiazines. Eur. J. Med. Chem. 2011;46:3179–89. doi: https://doi.org/10.1016/j.ejmech.2011.05.013.
[9] Prajna P, Bismita M, Deya NRK. PEGylation in anti-cancer therapy: An overview. Asian J. Pharm. Sci. 2016;11:337–48. doi: https://doi.org/10.1016/j.ajps.2015.08.011.
[10] Banerjee SS, Aher N, Patil R, Khandare J. Poly(ethylene glycol)-prodrug conjugates: concept, design, and applications. J. Drug Deliv. 2012;2012:1–17. doi: https://doi.org/10.1155/2012/103973.
[11] Cibotaru S, Sandu AI, Belei D, Marin L. Water soluble PEGylated phenothiazines as valuable building blocks for bio-materials. Mater. Sci. Eng. C. 2020;116:. doi: https://doi.org/10.1016/j.msec.2020.111216111216.
[12] O. A. Peña-Morán, M. L. Villarreal, L. Álvarez-Berber, A. Meneses-Acosta, V. Rodríguez-López, Cytotoxicity, Post-Treatment Recovery, and Selectivity Analysis of Naturally Occurring Podophyllotoxins from Bursera fagaroides var. fagaroides on Breast Cancer Cell Lines. Molecules, 21(2016) 1013. doi: 10.3390/molecules21081013.
[13] Son KD, Kim YJ. Anticancer activity of drug-loaded calcium phosphate nanocomposites against human osteosarcoma. Biomaterials Research21 2017:13. doi: https://doi.org/10.1186/s40824-017-0099-1.
[14] W.S. Rasband, ImageJ, U. S. National Institutes of Health, Bethesda, Maryland, USA, https://imagej.nih.gov/ij/, 1997–2018.
[15] Newell DR, Burtles SS, Fox BW, Jodrell DI, Connors TA. Evaluation of rodent-only toxicology for early clinical trials with novel cancer therapeutics. Br J Cancer. 1999;81:760–8. doi: https://doi.org/10.1038/sj.bjc.6690761.
[16] Workman P, Aboagye EO, Balkwill F, Balmain A, Bruder G, Chaplin DJ, et al. Guidelines for the welfare and use of animals in cancer research. Br J Cancer. 2010;102:1555–77. doi: https://doi.org/10.1038/sj.bjc.6605642.
[17] Goyette MA, Cusseddu R, Elkholi I, Abu-Thuraia A, El-Hachem N, Haibe-Kains B, et al. AXL knockdown gene signature reveals a drug repurposing opportunity for a class of antipsychotics to reduce growth and metastasis of triple-negative breast cancer. Oncotarget 2019;10:2055–67. doi: https://doi.org/10.18632/oncotarget.26725.
[18] Xu F, Xia Y, Feng Z, Lin W, Xue Q, Jiang J, et al. Repositioning antipsychotic fluphenazine hydrochloride for treating triple negative breast cancer with brain metastases and lung metastases. Am J Cancer Res 2019;9:. https://pubmed.ncbi.nlm.nih.gov/30949404/459478.
[19] Mary M, Tomayko C, Reynolds P. Determination of subcutaneous tumor size in athymic (nude) mice. Cancer Chemother. Pharmacol. 1989;24:148–54. doi: https://doi.org/10.1007/BF00300234.
[20] Dehsari HS, Ribeiro AH, Ersöz B, Tremel W, Jakob G, Asadi K. Effect of precursor concentration on size evolution of iron oxide nanoparticles. Cryst. Eng. Comm. 2017;19:6694–702. doi: https://doi.org/10.1039/C7CE01406F.
[21] Moghimipour E, Dorkoosh FA, Rezaei M, Ramezani Z, Amini M, Kouchak M, et al. Folic acid-modified liposomal drug delivery strategy for tumor targeting of 5-fluorouracil. Eur. J. Pharm. Sci. 2017;114:. doi: https://doi.org/10.1016/j.ejps.2017.12.011166174.
[22] Danhier F, Touan T, Kouhé B, Duhem N, Ucakar B, Staub A, et al. Vitamin E-based micelles enhance the anticancer activity of doxorubicin. Int. J. Pharm. 2014;476:9–15. doi: https://doi.org/10.1016/j.ijpharm.2014.09.028.
[23] X. F. Qi, D. H. Kim, Y. S. Yoon, S. K. Kim, D. Q. Cai, Y.C. Teng, K. Y. Shim, K. J. Lee Involvement of oxidative stress in simvastatin-induced apoptosis of murine CT26 colon carcinoma cells, Toxicol.Lett. 199 (2010) 277-287. doi: 10.1016/j.toxlet.2010.09.010
[24] Moghadam NH, Salehzadeh S, Tanzadehpanah H, Saidijam M, Karimi J, Khazalpour S. In vitro cytotoxicity and DNA/HSA interaction study of triamterene using molecular modelling and multi-spectroscopic methods. J. Biomol. Struct. Dyn. 2019;27:1–35. doi: https://doi.org/10.1080/07391102.2018.1489305.
[25] Li C, Chen C, An Q, Yang T, Sang Z, Yang Y, et al. A novel series of napabucasin derivatives as orally active inhibitors of signal transducer and activator of transcription 3 (STAT3). Eur. J. Med. Chem. 2019;162:543–54. doi: https://doi.org/10.1016/j.ejmech.2018.10.067.
[26] Tanzadehpanah H, Bahmani A, Moghadam NH, Gholami H, Mahaki H, Farmany A, et al. Synthesis, anticancer activity, and β-lactoglobulin binding interactions of multitargeted kinase inhibitor sorafenib tosylate (SORt) using spectroscopic and molecular modelling approaches. Luminescence 2020;36:117–28. doi: https://doi.org/10.1002/bio.3929.
[27] W.C. Lin, W.H. Wang, Y.H. Lin, J.D. Leu, S.Y. Cheng. Y.J. Chen, J.J. Hwang, Synergistic effects of tetrandrine combined with ionizing radiation on a murine colorectal carcinoma–bearing mouse model, Oncol. Rep. 40(2018) 1390-1400. doi: 10.3892/or.2018.6568
[28] Jeevarathinam AS, Lemaster JE, Chen F, Zhao E, Jokerst JV. Photoacoustic, Imaging Quantifies Drug Release from Nanocarriers via Redox Chemistry of Dye-Labeled Cargo. Angew. Chem. 2020;59:4678–83. doi: https://doi.org/10.1002/anie.201914120.
[29] Chiarante N, García Vior MC, Awruch J, Marino J, Roguin LP. Phototoxic action of a zinc(II) phthalocyanine encapsulated into poloxamine polymeric micelles in 2D and 3D colon carcinoma cell cultures. J Photochem Photobiol B. 2017;170:140–51. doi: https://doi.org/10.1016/j.jphotobiol.2017.04.009.
[30] Caneschi W, Enes KB, Carvalho de Mendonça C, Fernandes FS, Miguel FB, Martins J, et al. Synthesis and anticancer evaluation of new lipophilic 1,2,4 and 1,3,4-oxadiazoles. Eur. J. Med. Chem. 2019;165:18–30. doi: https://doi.org/10.1016/j.ejmech.2019.01.001.
[31] Shin MC, Zhang J, David AE, Trommer WE, Kwon YM, Min KA, et al. Chemically and biologically synthesized CPP-modified gelonin for enhanced anti-tumor activity. J. Control. Release 2013;172:169–78. doi: https://doi.org/10.1016/j.jconrel.2013.08.016.
[32] Moghimipour E, Rezaei M, Ramezani Z, Kouchak M, Amini M, Angal KA, et al. Folic acid-modified liposomal drug delivery strategy for tumor targeting of 5-fluorouracil. Eur. J. Pharm. Sci. 2018;114:166–74. doi: https://doi.org/10.1016/j.ejps.2017.12.011.
[33] J.D.S. Chaves, L.G. Tunes, C.H. de J. Franco, T.M. Francisco, C.C. Corrêa, S.M.F. Murta, M.V. de Almeida, Novel gold(I) complexes with 5-phenyl-1,3,4-oxadiazole-2-thione and phosphine as potential anticancer and antileishmanial agents, Eur. J. Med. Chem., 127 (2017) 727–739. doi: 10.1016/j.ejmech.2016.10.052
[34] M. Lopez-Lazaro, A Simple and Reliable Approach for Assessing Anticancer Activity In Vitro, Curr. Med. Chem., 22 (2015), 1324–1334. doi. 10.2174/0929867322666150209150639
[35] O. Peña-Morán, M. Villarreal, L. Álvarez-Berber, A. Meneses-Acosta, V. Rodríguez-López, Cytotoxicity, Post-Treatment Recovery, and Selectivity Analysis of Naturally Occurring Podophyllotoxins from Bursera fagaroides var. fagaroides on Breast Cancer Cell Lines. Molecules, 21(2018) 1013. doi:10.3390/molecules21081013
[36] Molecular Probes Handbook: A Guide to Fluorescent Probes and Labeling Technologies, 11th Edition, Life Technologies Corporation, 2010

[37] Elmore S. Apoptosis: a review of programmed cell death. Toxicol Pathol. 2007;35:495–516. doi: https://doi.org/10.1080/01926230701320337.
[38] J.H. Choi, Y.R. Yang, S.K. Lee. S.H. Kim. Y.H. Kim, J.Y. Cha. S.W. Oh, J.R. Ha. S.Ho, R.P.G. Suh, Potential inhibition of pdk1/akt signaling by phenothiazines suppresses cancer cell proliferation and survival, Ann. N. Y. Acad. Sci. 1138 (2008) 393–403 doi:10.1196/annals.1414.041
[39] Kuzu O, Gowda R, Noory M. Modulating cancer cell survival by targeting intracellular cholesterol transport. Br. J. Cancer. 2017;117:513–24. doi: https://doi.org/10.1038/bjc.2017.200.
[40] Seelig A, Gottschlich R, Devant RM. A method to determine the ability of drugs to diffuse through the blood-brain barrier. Proc. Natl. Acad. Sci. USA 1994;91:68–72. doi: https://doi.org/10.1073/pnas.91.1.68.
[41] Al Shoyaib A, Archie SR, Karamyan VT. Intraperitoneal route of drug administration: should it be used in experimental animal studies? Pharm. Res. 2019;37:12. doi: https://doi.org/10.1007/s11095-019-2745-x.
[42] Jiang X, Chen Z, Shen G, Jiang Y, Wu L, Li X, et al. Psychotropic agent thioridazine elicits potent *in vitro* and *in vivo* antimelanoma effects. Biomed Pharmacother 2018;97:833–7. doi: https://doi.org/10.1016/j.biopha.2017.11.012.
[43] Lee SJ, Jeong Y, Park H, Kang DH, Oh J, Lee S, et al. Enzyme-responsive doxorubicin release from dendrimer nanoparticles for anticancer drug. Int J Nanomed 2015;10:5489–503. doi: https://doi.org/10.2147/IJN.S87145.
[44] Pangeni R, Choi SW, Jeon OC, Byun Y, J.W.. ParkMultiple nanoemulsion system for an oral combinational delivery of oxaliplatin and 5-fluorouracil: preparation and in vivo evaluation. Int J Nanomed 2016;11:6379–99. doi: https://doi.org/10.2147/IJN.S121114.
[45] Kageyama Y, Yamazaki Y, Okuno H. Novel approaches to prodrugs of anticancer diaminodichloroplatinum(II) complexes activated by stereoselective enzymatic ester hydrolysis. J Inorg Biochem. 1994;70:25–32. doi: https://doi.org/10.1016/S0162-0134(98)00009-9.
[46] Dagher Z, Borgie M, Magdalou J, Chahine R, Greige-Gerges H. p-Hydroxybenzoate esters metabolism in MCF7 breast cancer cells. Food Chem. Toxicol. 2012;50:4109–14. doi: https://doi.org/10.1016/j.fct.2012.08.013.
[47] Dong H, Pang L, Cong H, Shen Y, Yu B. Application and design of esterase-responsive nanoparticles for cancer therapy. Drug Delivery 2019;26:416–32. doi: https://doi.org/10.1080/10717544.2019.1588424.
[48] Belei D, Dumea C, Samson A, Farce A, Dubois J, Bîcu E, et al. New farnesyltransferase inhibitors in the phenothiazine series Bioorg. Med. Chem. Lett. 2012;22:4517–22. doi: https://doi.org/10.1016/j.bmcl.2012.06.007.
[49] Abuhaie CM, Ghinet A, Farce A, Dubois J, Gautret P, Rigo B, et al. Synthesis and biological evaluation of a new series of phenothiazine-containing protein farnesyltransferase inhibitors. Eur. J. Med. Chem. 2013;59:101–10. doi: https://doi.org/10.1016/j.ejmech.2012.11.008.
[50] Haluska P, Dy G, Adjei A. Farnesyl transferase inhibitors as anticancer agents. Eur. J. Cancer 2002;38:1685–700. doi: https://doi.org/10.1016/S0959-8049(02)00166-1.
[51] Dumitriu GM, Bîcu E, Belei D, Rigo B, Dubois J, Farce A, et al. Phenothiazine-based CaaX competitive inhibitors of human farnesyltransferase bearing a cysteine, methionine, serine or valine moiety as a new family of antitumoral compounds. Bioorg. Med. Chem. Lett. 2015;25:4447–52. doi: https://doi.org/10.1016/j.bmcl.2015.09.008.
[52] Bejan A, Doroftei F, Cheng X, Marin L. Phenothiazine-chitosan based eco-adsorbents: A special design for mercury removal and fast naked eye detection. Int. J. Biol. Macromol. 2020;162:1839–48. doi: https://doi.org/10.1016/j.ijbiomac.2020.07.232.
[53] Mishra P, Nayak B, Dey RK. PEGylation in anti-cancer therapy: An overview. Asian J. Pharm. Sci. 2006;11:337–48. doi: https://doi.org/10.1016/j.ajps.2015.08.011.
[54] Bejan A, Marin L. Phenothiazine based nanocrystals with enhanced solid state emission. J Mol Liq 2018;265:299–306. doi: https://doi.org/10.1016/j.molliq.2018.05.125.
[55] Marin L, Bejan A. Phenothiazine based co-crystals with enhanced luminescence. Dyes and Pigments 175 2020:. doi: https://doi.org/10.1016/j.dyepig.2019.108164108164.
[56] Shen Z, Ye H, Kröger M, Li Y. Aggregation of polyethylene glycol polymers suppresses receptor-mediated endocytosis of PEGylated liposomes Nanoscale 2018;10:4545–60. doi: https://doi.org/10.1039/c7nr09011k.
[57] Zhang L, Shi D, Shi C, Kaneko T, Chen M. Supramolecular micellar drug delivery system based on multi-arm block copolymer for highly effective encapsulation and sustained-release chemotherapy. J. Mater. Chem. B. 2012;2009:1–3. doi: https://doi.org/10.1039/C9TB01221D.